Old Dominion University
ODU Digital Commons

Electrical & Computer Engineering Faculty Publications

Electrical & Computer Engineering

2008

Activation Energy of Surface Diffusion and Terrace Width Dynamics During the Growth of in (4×3) on Si (100) - (2×1) by Femtosecond Pulsed Laser Deposition

M. A. Hafez
Old Dominion University

H. E. Elsayed-Ali
Old Dominion University, helsayed@odu.edu

Follow this and additional works at: http://digitalcommons.odu.edu/ece_fac_pubs

Part of the Atomic, Molecular and Optical Physics Commons, Electrical and Computer Engineering Commons, Physical Chemistry Commons, and the Semiconductor and Optical Materials Commons

Repository Citation
Hafez, M. A. and Elsayed-Ali, H. E., "Activation Energy of Surface Diffusion and Terrace Width Dynamics During the Growth of in (4×3) on Si (100) - (2×1) by Femtosecond Pulsed Laser Deposition" (2008). *Electrical & Computer Engineering Faculty Publications*. 99.
http://digitalcommons.odu.edu/ece_fac_pubs/99

Original Publication Citation
Hafez, M. A., & Elsayed-Ali, H. E. (2008). Activation energy of surface diffusion and terrace width dynamics during the growth of in (4×3) on Si (100) - (2×1) by femtosecond pulsed laser deposition. *Journal of Applied Physics, 103*(9), 093510. doi:10.1063/1.2909923

This Article is brought to you for free and open access by the Electrical & Computer Engineering at ODU Digital Commons. It has been accepted for inclusion in Electrical & Computer Engineering Faculty Publications by an authorized administrator of ODU Digital Commons. For more information, please contact digitalcommons@odu.edu.

Activation energy of surface diffusion and terrace width dynamics during the growth of In(4×3) on Si(100)-(2×1) by femtosecond pulsed laser deposition

M. A. Hafez and H. E. Elsayed-Ali[a)]
Department of Electrical and Computer Engineering and the Applied Research Center, Old Dominion University, Norfolk, Virginia 23529, USA

(Received 24 January 2008; accepted 6 March 2008; published online 5 May 2008)

The nucleation and growth of indium on a vicinal Si(100)-(2×1) surface at high temperature by femtosecond pulsed laser deposition was investigated by *in situ* reflection high energy electron diffraction (RHEED). RHEED intensity relaxation was observed for the first ∼2 ML during the growth of In(4×3) by step flow. From the temperature dependence of the rate of relaxation, an activation energy of 1.4±0.2 eV of surface diffusion was determined. The results indicate that indium small clusters diffused to terrace step edges with a diffusion frequency constant of $(1.0\pm0.1)\times10^{11}$ s^{-1}. The RHEED specular beam split peak spacing, which is characteristic of a vicinal surface, was analyzed with the growth temperature to obtain the average terrace width. Gradual reduction in the terrace width during growth of In(4×3) was observed with In coverage and is attributed to the detachment of In atoms from terrace edges. At a substrate temperature of 405 °C, the average terrace width decreased from 61±10 Å, which corresponds to the vicinal Si(100) surface, to an equilibrium value of 45±7 Å after deposition of ∼23 ML. Further In coverage showed a transition of the RHEED pattern from (4×3) to (1×1) and the growth of rounded In islands (average height of ∼1 nm and width of ∼25 nm), as examined by *ex situ* atomic force microscopy. © *2008 American Institute of Physics*. [DOI: 10.1063/1.2909923]

I. INTRODUCTION

The growth of In on Si(100)-(2×1) surfaces induces different surface reconstructions depending on the In coverage and the substrate temperature (T_s). The growth of In on Si(100)-(2×1) at high temperatures results in the formation of a well ordered In(4×3) superlattice.[1–4] For an In coverage of ∼0.15 ML [1 ML=6.8×10^{14} atoms/cm^2 for the unreconstructed Si(100) surface], the In(4×3) surface grown on Si(100)-(2×1) at 500 °C was identified to be composed of nearly identical-size nanoclusters that were randomly distributed. The In(4×3) surface became ordered arrays at an ∼0.5 ML In coverage.[5] The structural and electronic properties of these nanoclusters show that they have the potential for future nanoscale and electronic device applications.[6–9]

The In(4×3) surface was studied by Auger electron spectroscopy, reflection high-energy electron diffraction (RHEED), low energy electron diffraction (LEED), scanning tunneling microscopy (STM), impact-collision ion-scattering spectrometry, and x-ray diffraction.[1–4,10–14] The In(4×3) structural model has been a subject of debate. Theoretical and experimental studies using first principles total energy calculations, STM image simulations, and photoelectron holography were performed to solve the structural model of the In(4×3) on Si(100).[15–17] Their results favored the x-ray diffraction analysis by Bunk *et al.*,[13] in which the 4×3 unit cell comprises a stable pyramidlike Si_7In_6 cluster. The results showed that the initial structure is a mix of In(4×3) and Si(2×1) until the surface becomes fully In(4×3) at a coverage of 0.5 ML. By using STM, Baski *et al.*[4] suggested that the growth of the In(4×3) at 0.5 ML In is accompanied by the displacement of the underlying Si surface atoms. Knall *et al.*[2,3] grew In on nominally flat Si(100)-(2×1) surfaces by molecular beam epitaxy (MBE) and observed the In(4×3) phase by RHEED and LEED for T_s=150–600 °C. For In coverages >2 ML, the (4×3) surface was decorated with three-dimensional (3D) islands or replaced by a disordered phase. This transition between the (4×3)+3D island morphology to a disordered two-dimensional (2D) layer +3D islands occurred as T_s was raised above ∼450 °C. Scanning electron microscopy (SEM) showed hemispherical-shaped islands grown on the In(4×3) surface at 15 ML of In. Changes in surface morphology that are induced by the adsorption of In on Si(100)-(2×1) surfaces were studied by STM and low energy electron microscopy (LEEM).[18,19] The (4×3) structure was found to transform to a (4×1) structure when the Si(100)-In(4×3) surface was exposed to atomic hydrogen at 300 °C and at room temperature.[20,21] In addition, the film morphology was changed from 2D layers to In clusters.

Compared to MBE and conventional evaporation sources, pulsed laser deposition (PLD) produces highly energetic species with high instantaneous deposition rates.[22] The energetic species in PLD increases the deposit surface diffusion and promotes epitaxy. The high nucleation density of deposits in PLD improves 2D growth, and this property led to the growth of high quality metallic thin films.[23,24] An imposed 2D growth mode due to the pulsed nature of PLD followed by a relaxation time was demonstrated.[25] RHEED

[a)]Electronic mail: helsayed@odu.edu.

 © 2008 American Institute of Physics

intensity modulation by each deposition laser pulse was used to estimate the surface diffusion parameters.[26] While most published studies focused on the determination of surface phases induced by a submonolayer of In on Si, the kinetic parameters and morphology changes during the growth of In(4×3) need further study. The growth of In on Si(100) by femtosecond PLD at high temperatures can be used to investigate the effect of PLD characteristics on the growth mode and kinetics of In(4×3) formation.

We have studied femtosecond PLD of In on a vicinal Si(100)-(2×1) surface within the temperature range of 350–420 °C. RHEED was used to probe the growth dynamics of In(4×3) on Si(100)-(2×1). The film morphology was examined *ex situ* by atomic force microscopy (AFM) and STM. The activation energy and diffusion frequency for the formation of In(4×3) were estimated from the RHEED intensity relaxation at an In coverage of ~0.5 ML. The terrace width dynamics was studied at different deposition conditions to investigate the associated surface processes during the growth of In(4×3). The variation in the average terrace width with In coverage and its effect on the growth mode and morphology were examined.

II. EXPERIMENT

The growth was performed in an ultrahigh-vacuum (UHV) PLD system. The base pressure during deposition was in the low 10^{-9} Torr range. An amplified Ti:sapphire laser [pulse width ~130 fs full width at half maximum (FWHM)], operating at a wavelength of 800 nm and at a repetition rate within the range of 1–50 Hz, was used to ablate the In target. The laser was incident on a 99.99% pure In target at ~45° and focused on the In target by using a convex lens with a 30 cm focal length. The target was rotated at a speed of 2 rpm in order to minimize particulate formation. The target-to-substrate distance was fixed at ~5 cm. RHEED was used to observe the surface structure of the substrate and the film growth during deposition. The RHEED electron gun was operated at an electron energy of 8.6 keV. A charge-coupled device camera was used to image the diffraction patterns. Real-time evaluation of the intensity and FWHM of the RHEED beams were performed and correlated with the deposition conditions. RHEED analyses along and across the diffracted beams were obtained in the reciprocal space and then converted to length scales after taking into account the instrumental response. The uncertainties in the electron energy and the RHEED camera length were determined by measuring the in-plane lattice parameter of the Si(100) surface. The surface morphology of the In films was imaged and characterized *ex situ* with noncontact AFM and STM.

The ~5×10 mm Si substrates were cut from a low-resistivity Si(100) wafer (*p* type, boron doped, 500 μm thick, and 0.01–0.03 Ω cm resistivity). The Si surfaces were misoriented from the low-index (100) plane by 1.0° toward ⟨110⟩±0.5°. The Si(100)-(2×1) surface was prepared by chemical etching just prior to being loaded into the UHV chamber. This was followed by *in situ* heat cleaning to 600 °C for several hours by using a direct current, then flash heating at ~1100 °C to remove native oxides and carbon. Just prior to In deposition, Si(100)-(2×1) was raised in temperature to ~1000 °C for ~2 min by direct-current heating. During flash heating of the substrate, the chamber pressure was in the low 10^{-8} Torr. The heating was then terminated, and the substrate cooled down to the growth temperature. RHEED patterns acquired after annealing were characteristic of clean reconstructed Si(100)-(2×1).

Calibration of the deposition rate per laser pulse was accomplished by using the phenomenon of RHEED intensity oscillations, which provides a highly accurate method of obtaining the film thickness. RHEED oscillations were observed at substrate temperatures near the melting point of In. Thus, we performed several depositions at this condition to observe RHEED oscillations. The deposition rate was estimated to be ~0.05 ML/pulse. This was confirmed by a post-deposition estimate of film thickness by using a profilometer.

III. RESULTS AND DISCUSSION

A. Growth of In(4×3) on Si

The growth of In on the vicinal Si(100)-(2×1) surface was performed at different deposition conditions. Figures 1(a) and 1(b) show the RHEED patterns of clean Si(100)-(2×1) surface before deposition that were taken along the [011] and $[0\bar{1}\bar{1}]$ azimuths, down and up the staircase, respectively. Short streaks in the RHEED Laue semicircles and Kikushi lines were visible. For In growth at T_s within the range of 350–420 °C, the RHEED pattern began to change from that characteristic of the initial Si(100)-(2×1) reconstruction to that of the In(4×3) reconstruction at a coverage of ~0.5 ML of In. Figures 1(c) and 1(d) show the RHEED patterns of the In(4×3) superstructure on Si(100)-(2×1) in the [011] and $[0\bar{1}\bar{1}]$ azimuths, respectively. The laser was operated at a 2 Hz repetition rate with an energy density of 0.50 J/cm^2. The In(4×3) RHEED patterns show streaky integral and fractional orders with sharp spots, indicating a smooth and high quality epitaxial In film. It was noticed that the Si(100)-(2×1) RHEED pattern improved when In was deposited on Si at lower than 500 °C and then desorbed by heating the Si surface at ~1000 °C. After In desorption and cooling the substrate, the diffracted spots became more pronounced at the higher Laue zones with less background on the RHEED screen. This was observed to considerably enhance the appearance of the In(4×3) structure with subsequent In deposition. This is consistent with a previous study, which reported that In can be evaporated on a hot Si surface in UHV to eliminate native oxide without indiffusion of In and introduction of surface defects into Si during the desorption process.[27]

Figure 2 shows the RHEED intensity of the specular beam during the growth of In at T_s=400 °C. The laser was operated at a 50 Hz repetition rate and an energy density of 0.07 J/cm^2. At these deposition conditions, the In(4×3) was still observable for ~50 s after starting the deposition. With increasing In coverage, a continuous increase in the RHEED background intensity was observed, and the (4×3) RHEED pattern was replaced by a streaky (1×1) pattern. Knall *et al.*[3] reported that at temperatures less than

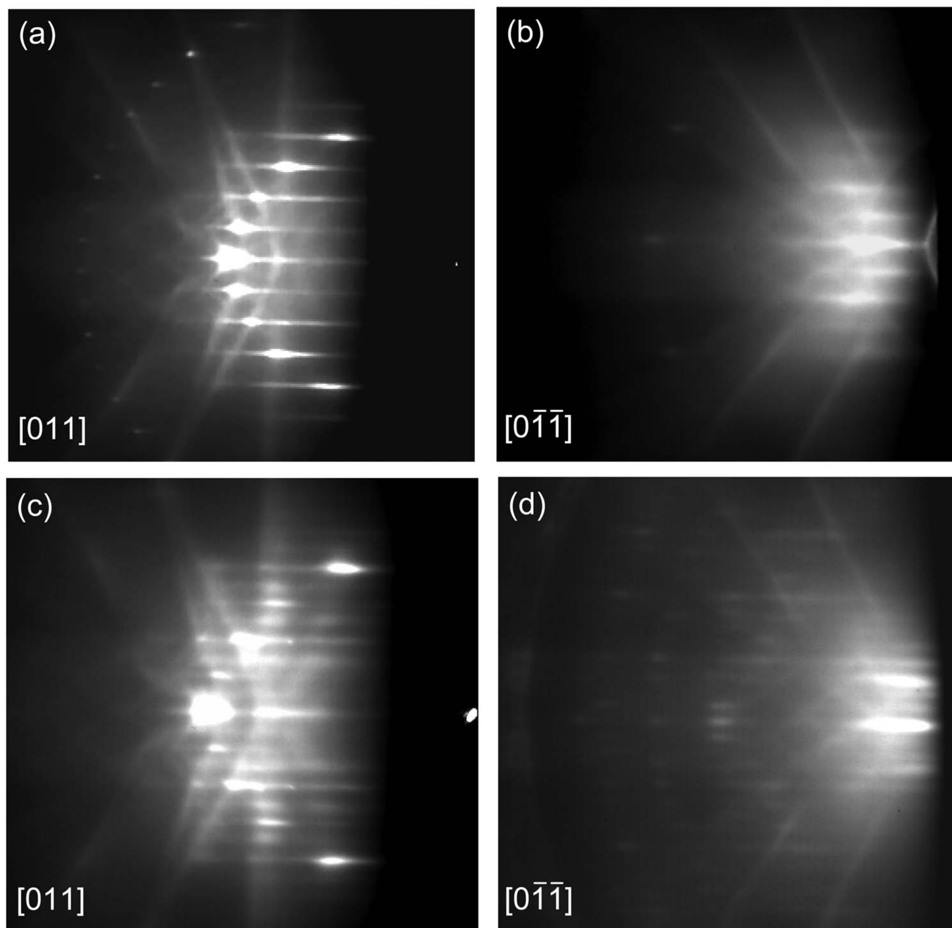

FIG. 1. [(a) and (b)] RHEED patterns of Si(100)-(2×1) surface before In deposition taken along the [011] and [0$\bar{1}\bar{1}$] azimuths, respectively. [(c) and (d)] RHEED patterns of In(4×3) grown on Si(100)-(2×1) by femtosecond PLD taken along the [011] and [0$\bar{1}\bar{1}$] azimuths, respectively. The laser was operated at a 2 Hz repetition rate with an energy density of 0.50 J/cm^2 on the In target.

450 °C, only a continuous decrease of the diffraction spots and weak In(4×3) RHEED and LEED patterns were still visible at 1000 ML of In, which is the highest coverage used in their experiment, indicating a 3D growth on top of the In(4×3) layer. In our case, the high RHEED background

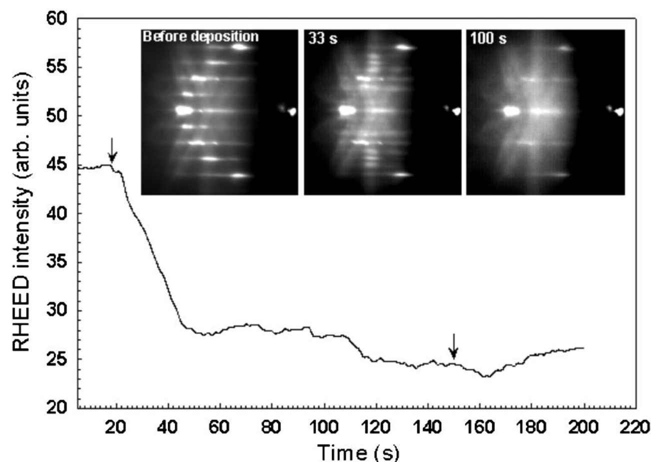

FIG. 2. RHEED intensity of the specular beam during growth of In at a substrate temperature of 400 °C. The laser was operated at a 50 Hz repetition rate and an 0.07 J/cm^2 laser energy density on the In target. The surface structure changed successively from (2×1) to (4×3) then to (1×1) after ~1500 laser shots, as shown in the inset RHEED patterns. The RHEED patterns are taken in the [011] azimuth before and during In deposition for 33 and 100 s. The arrows indicate the time at which the ablating laser was turned on and off.

indicated the growth of In islands on the surface. As growth proceeded, shadowing of the incident electron beam by the islands decreased reflections from the In(4×3) underlayer and caused a reduction in the specular beam intensity. For laser energy densities on the In target in the range of 0.07–0.50 J/cm^2, the transition from Si(100)-(2×1) to In(4×3) reconstruction was followed by a transformation to the (1×1) pattern with increasing In coverage. We did not observe bulk transmission diffraction features in RHEED throughout the entire deposition conditions. The morphology of the grown In films was examined *ex situ* by using AFM. Figure 3(a) shows an AFM image of an In film grown on Si(100)-(2×1) at 386 °C at a coverage of ~38 ML of In. At this coverage, the In(4×3) RHEED pattern was still observable but had a higher background as the In coverage was increased. The laser was operated at a 2 Hz repetition rate and the energy density on the In target was 0.50 J/cm^2. The AFM image shows In islands of almost identical sizes grown on the surface. Figure 3(b) shows a line scan taken over an In island with a rounded shape that is characterized by a height of ~1 nm and a width of ~25 nm. Figure 3(c) is a 3D STM image of the film morphology, which shows In islands of comparable shapes and sizes distributed over the surface. In a previous MBE growth of In on Si(100)-(2×1), SEM images showed hemispherical In islands of an average diameter of 300 nm with a minimum separation of 500 nm between islands at a film coverage of 15 ML.[2] The streaky (1×1) RHEED pattern, as shown in Fig. 2 at 100 s, and the AFM

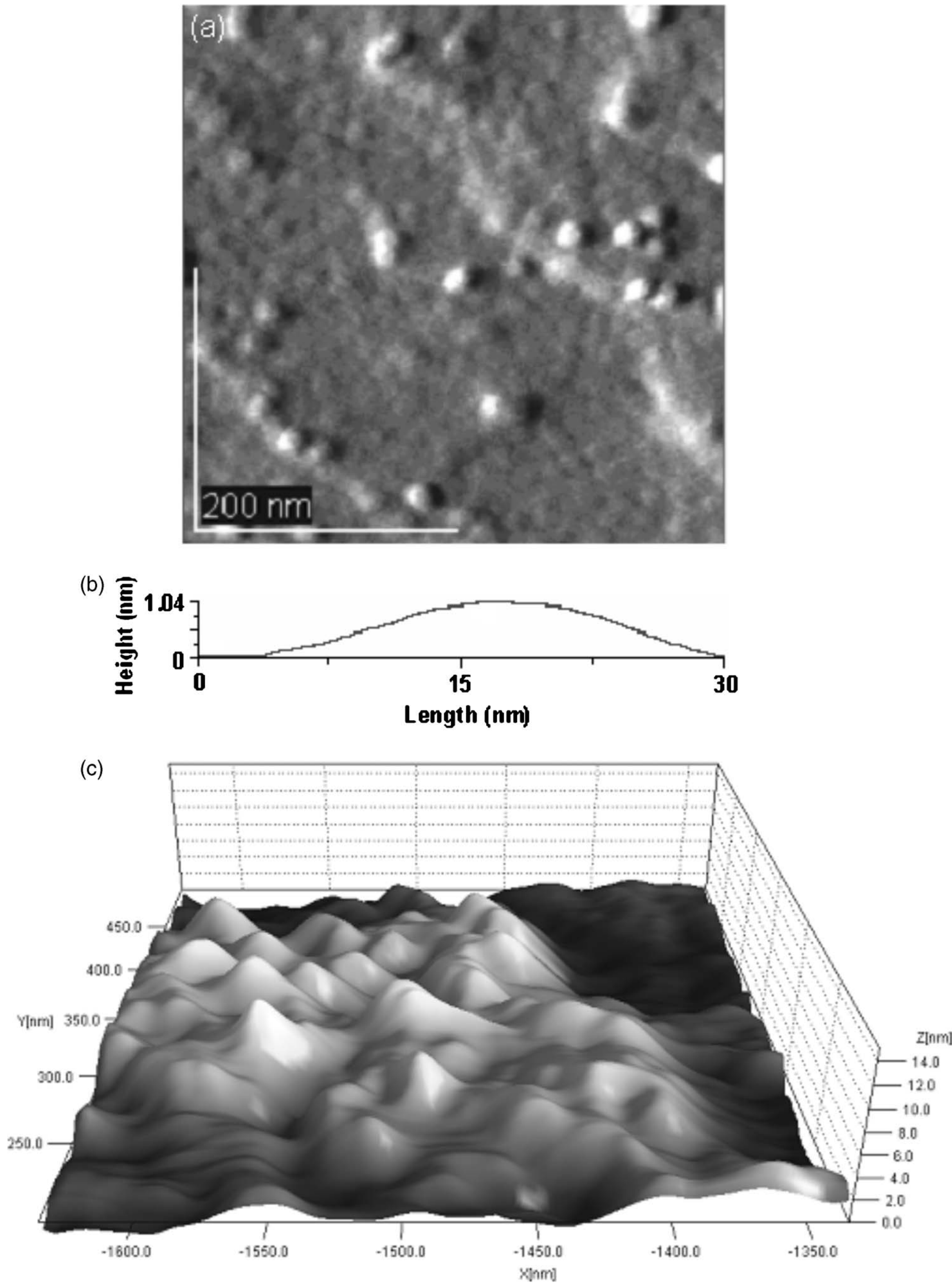

FIG. 3. (a) AFM image of the grown In film on Si(100)-(2×1) at 386 °C for an In coverage of ~38 ML. The laser was operated at a 2 Hz repetition rate and the laser energy density was 0.50 J/cm^2 on the In target. (b) Line profile of an In island shows a rounded shape with a height of ~1 nm and a width of ~25 nm. (c) 3D STM image of the In film morphology showing grown islands.

profile indicate the growth of In 2D rounded islands on top of the In(4×3) surface. The rounded shape of the islands show that the In deposits have an isotropic growth on the In(4×3) surface compared to the In(2×1) surface structure that forms on Si(100)-(2×1) at room temperature, where an anisotropic growth leads to the formation of elongated In islands.[2,28]

Next, the RHEED intensity was monitored to determine the growth mode and kinetic parameters associated with the formation of the initial In(4×3) structure in the femtosecond PLD of In on Si(100)-(2×1). Figure 4 shows the specular beam RHEED intensity during the growth of In(4×3) on Si(100)-(2×1) at T_s=390 °C. The laser was operated at a 2 Hz repetition rate with an energy density of 0.50 J/cm^2 on the In target. In the first ~1 ML, the RHEED intensity relaxes between the deposition laser pulses. After terminating In deposition, recovery of the RHEED intensity to its initial value was observed. The inset in Fig. 4 shows a similar behavior of the RHEED intensity for In film deposited at T_s =400 °C and 0.37 J/cm^2 ablating laser energy density.

B. RHEED intensity relaxation and activation energy

Deposition of In on Si(100)-(2×1) was performed at T_s within the range of 386–405 °C and the growth was monitored by RHEED. For an In coverage of ~6 ML, the RHEED intensities showed full recovery after growth termination similar to Fig. 4. Figure 5 shows the RHEED specular peak intensity during the growth of the first ~2 ML of In at different T_s. These films were grown with a total coverage of ~6 ML. The laser was operated at a 2 Hz repetition rate with an energy density of 0.50 J/cm^2 on the In target. The primary electron beam was incident along the [011] azimuth,

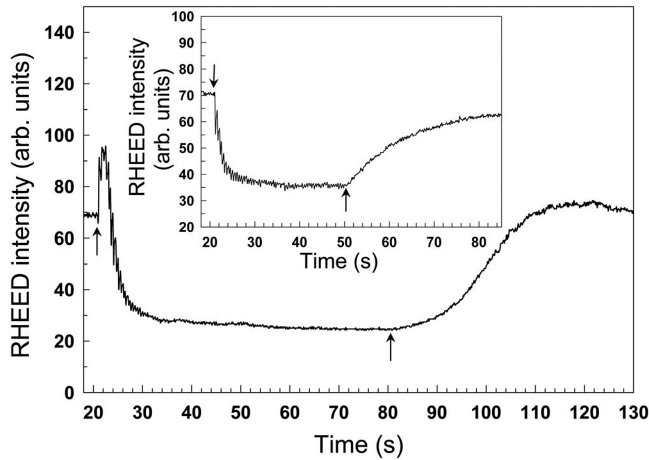

FIG. 4. RHEED intensity of the specular beam during the growth of In on Si(100)-(2×1) by femtosecond PLD. The In film was grown at a substrate temperature of 390 °C at a 2 Hz laser repetition rate and an energy density of 0.50 J/cm^2 on the In target. The specular beam intensity is shown in the inset for an In film grown at 400 °C by using a 2 Hz laser repetition rate and an energy density of 0.37 J/cm^2 on the In target. Recovery of the RHEED intensity occurred after termination of the deposition. The arrows indicate the time at which the ablating laser was turned on and off.

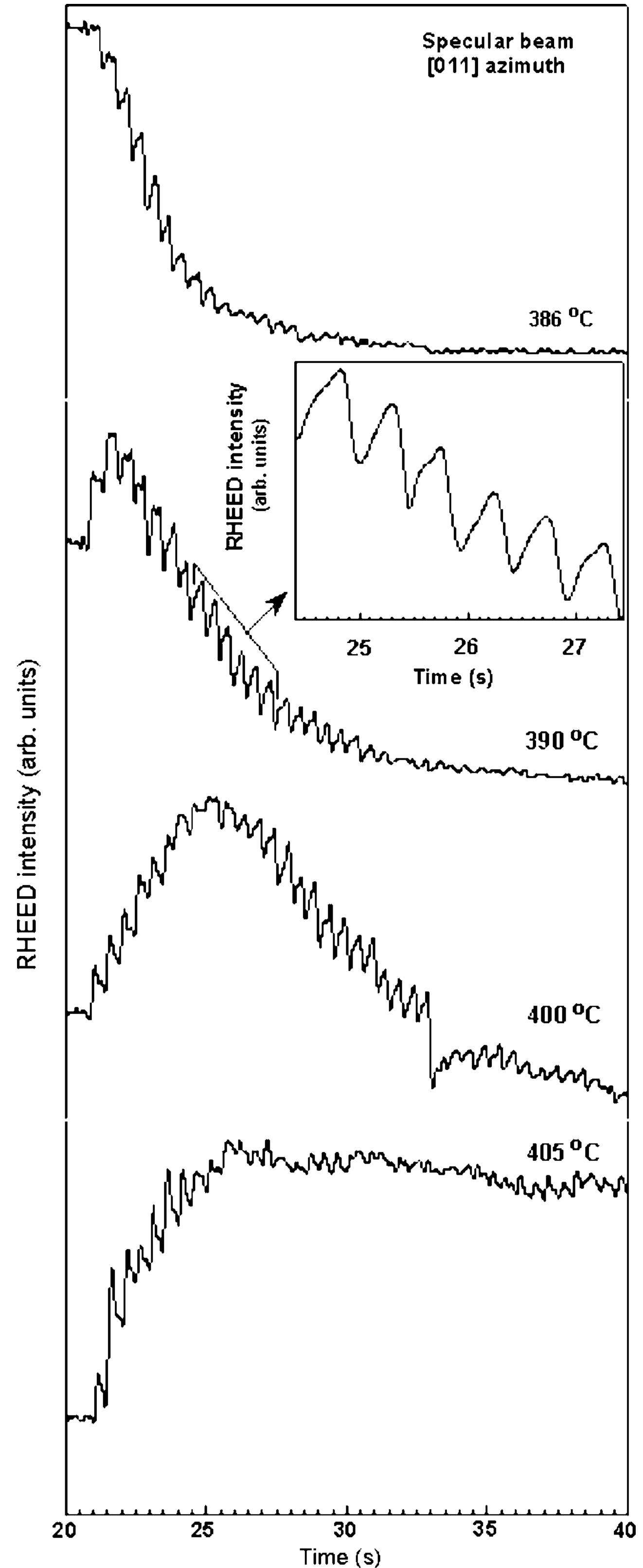

FIG. 5. RHEED intensity of the specular beam was monitored during growth of In within the first ~2 ML at different substrate temperatures. The laser was operated at a 2 Hz repetition rate with an energy density of 0.50 J/cm^2 on the In target. The primary electron beam was incident along the [011] azimuth down the staircase of the vicinal Si surface. The inset shows a magnified time scale of RHEED intensity relaxation observed after laser pulses during femtosecond PLD of In on Si(100) at T_s of 390 °C from the 6th to the 11th laser pulse.

down the staircase of the vicinal Si surface. At T_s=386 °C, the RHEED specular beam intensity decreased and reached a steady value after deposition of ~1 ML, whereas for T_s =390 and 400 °C, the specular beam intensity increased, initially reaching a peak value, then decreased with deposition time. The increase in the specular beam intensity was higher at T_s=400 °C compared to that at 390 °C. At T_s =405 °C, the specular beam intensity increased to a peak value in the first ~0.5 ML, reaching almost a flat peak that slowly decreased with further deposition. RHEED intensity relaxations were observed in the early stages of the growth of In(4×3) up to the first ~2 ML. The relaxations of the RHEED intensity indicate that surface smoothing took place between pulses during the In growth. The In(4×3) RHEED pattern showed sharp spots lying on the RHEED zeroth Laue semicircle similar to Fig. 1(c). The smoothing of the growth is attributed to the energetic effect of the incident In deposits on the substrate surface. The inset of Fig. 5 shows a magnified RHEED intensity of the specular beam for the 6th to the 11th laser pulses during In deposition at T_s=390 °C. The RHEED intensity oscillates with a period corresponding to the laser pulse repetition rate of 2 Hz. Each laser pulse ablating the In target deposits ~3.4×10^{13} atom/cm^2 of In on the surface. This causes the specularly reflected RHEED intensity to instantaneously decrease because of the increased random distribution of the incoming In deposits on the surface. Then, the deposited In atoms and the formed clusters rearrange on the surface, leading to the increased RHEED specular intensity until the arrival of the next In flux. During femtosecond PLD of In on Si, the surface smoothness changed with each laser pulse in a periodic fashion, which can be viewed as a kind of interrupted growth. In contrast, due to the continuous nature of MBE, this feature does not appear. The RHEED intensity relaxations between laser pulses during growth of In were observed to decay after deposition of the first ~2 ML of In.

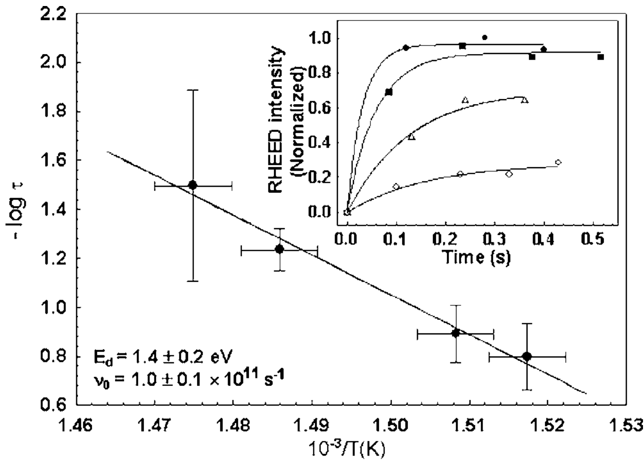

FIG. 6. The RHEED intensity relaxation measured at different growth temperatures. The inset shows the time dependence of the normalized RHEED intensity taken after the eighth laser deposition pulse, for a coverage of ~0.5 ML of In. The solid lines are exponential fit. The time constant τ has an Arrhenius temperature dependence. The activation energy E_d and the diffusion frequency constant ν_0 of the surface diffusion are determined.

The surface morphology prior to the deposition influenced the growth mode. For the vicinal Si(100)-(2×1) surface, the nucleation sites, such as vacancies and kinks, are located at terrace step edges at which atoms have lower coordination, making them more reactive. A RHEED investigation showed that the In surface segregation strength is reduced on vicinal substrates due to the effect of surface steps.[29] It was shown that no RHEED intensity relaxation takes place after each laser pulse when the growth mode is 2D layer by layer, while RHEED intensity relaxation is observed when the growth mode is step flow.[30] Step flow growth in PLD was previously observed and showed relaxation of RHEED intensity after each laser pulse.[30,31] The RHEED specular beam intensity development in Figs. 4 and 5 is indicative of step flow growth. No RHEED oscillations characteristic of layer-by-layer growth were observed. Moreover, the recovery of the specular spot intensity after growth termination observed in Fig. 4 rules out the increased surface roughness associated with columnar growth. The amount of In deposited in a single pulse, 0.05 ML/pulse, was much smaller than what was needed to grow a single monolayer. Depending on surface diffusion energy, the deposits diffused on the surface reaching terrace step edges.

The RHEED intensity relaxation depends on the growth temperature, as shown in Fig. 6. The time dependence of the normalized RHEED intensity for different T_s is shown in the inset of Fig. 6. The RHEED relaxation intensities were taken after the eighth laser pulse, for an In coverage of ~0.5 ML, for each deposition temperature. The relaxations have a rise that is well described by a single exponential in the form $I(t)=A[1-\exp(-t/\tau)]$, where A is a constant and τ represents a time constant for intensity rise. From the curve fits to the RHEED intensity, the time constant τ was found to decrease from 0.10 to 0.03 s for T_s of 386 and 405 °C, respectively. The characteristic time constant τ of the RHEED intensity relaxation following a laser pulse is related to the activation energy of surface diffusion by $1/\tau=\nu_0\exp(-E_d/k_BT_s)$, where ν_0 is the diffusion frequency constant, E_d is the activation energy, and k_B is Boltzmann's constant. The time constant τ has an Arrhenius temperature dependence, as shown in Fig. 6. The data are plotted in a log τ versus $1/T_s$ scale. A least-squares fit is used to yield E_d and ν_0. The activation energy E_d of the surface diffusion for In(4×3) on Si(100)-(2×1) by femtosecond PLD was 1.4 ± 0.2 eV. The diffusion frequency ν_0 measured from the plot is $(1.0\pm0.1)\times10^{11}$ s^{-1}. The vertical and horizontal error bars in the Arrhenius plot represent the statistical error and systematic uncertainty in the temperature measurements.

In general, the thin film growth mechanism depends on the deposition conditions, such as the deposition rate, the incident atom energy, and the surface condition. The activation energy depends on these various parameters. In the growth of superconducting thin films by PLD, an activation energy of 0.7 ± 0.1 eV for the diffusion of material units was estimated from the RHEED intensity oscillations.[26,32] The growth of homoepitaxial $SrTiO_3$ thin films by PLD at high temperatures (900–1380 °C) showed RHEED intensity modulation at the laser pulse repetition rate. Activation energies of the surface diffusion of 3.8 ± 0.3 and 3.3 ± 0.2 eV were estimated from the slow surface recovery after growth termination.[31] Such large activation energies were associated with detaching unit cells from kink sites at the edge of small islands.[31] In a MBE study of In on GaAs, the activation energy for the migration of In adatoms, at a temperature of 450–530 °C, was reported to be 1.6 eV.[33] The activation energy of surface diffusion for the growth of In(4×3) on Si(100)-(2×1) has not been previously reported. Both the energy of the ejected material from the In target and the substrate temperature influence the In(4×3) film growth process. The substrate temperature can affect the mobility of deposits on the surface. According to a Monte Carlo simulation of PLD, the incident particles' kinetic energies can play a similar role in film growth as the increase in substrate temperature.[34] The influence of the former on the activation energy is complex due to the interaction between the incident particles and the surface atoms.[34] Femtosecond PLD is known to result in the formation of a plume containing energetic species.[35] The growth of In on Si(100)-(2×1) by femtosecond PLD at room temperature showed the formation of the initial In(2×1) layer instead of an In(2×2) layer, as in MBE growth. The In(2×1) is formed by removing the reconstruction of Si(100)-(2×1) surface because of the energetic effect of the In species. This process affects the development of the film morphology.[28] Surface diffusion to the terrace step edges is influenced by the high kinetic energy of In deposits and the local surface lattice heating. The inelastic energy transfer from different In plume species to the surface causes surface lattice heating, enhancing surface diffusion.

The diffusion parameters during the growth of the In(4×3) layers depend on the type of the diffusing species. The diffusion frequency ν_0 of the adatoms over a surface is known to be in the range of 10^{13} s^{-1} (the vibrational frequency).[32] During the growth of In(4×3) by femtosecond PLD, the diffusion frequency constant determined from the Arrhenius plot $\nu_0=(1.0\pm0.1)\times10^{11}$ s^{-1} is two orders of magnitude lower than that for adatoms. This indicates that the rate limiting process is due to the surface diffusion of

clusters rather than of adatoms. The kinetics of In growth can be explained by the energetic and pulsed nature of PLD. The plume species that are mainly In atoms reach the surface and initially occupy disordered sites. The high instantaneous deposition rate results in a high nucleation density on the surface. Subsequently, the In atoms form small clusters that diffuse on the surface before they reach the terrace step edges. The diffusion frequency constant ν_0, which is obtained from RHEED intensity relaxation, is that of cluster diffusion. Previous experimental observations of fast diffusion of clusters and 2D island diffusion on surfaces were reported.[36–38] In a proposed model of heteroepitaxy by PLD, a diffusion frequency constant of 10^7 s^{-1} was obtained and referred to as the diffusion of material units rather than adatoms.[32] For the In(4×3) growth on vicinal Si(100)-(2×1) by femtosecond PLD, formation of small In clusters occurred during the high supersaturation period of a deposition pulse followed by surface diffusion of the small clusters to surface step edges with $E_d = 1.4 \pm 0.2$ eV.

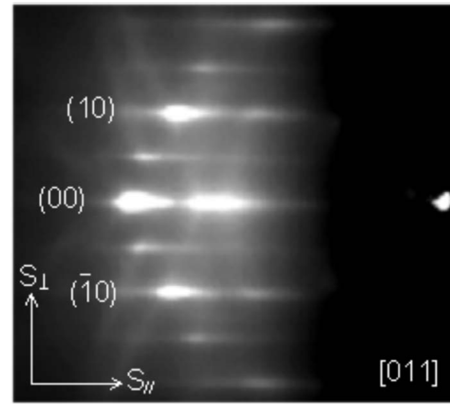

FIG. 7. RHEED pattern of the vicinal Si(100)-(2×1) surface taken at the out-of-phase condition corresponding to $\theta_{inc} \sim 65$ mrad. The primary electron energy of 8.6 keV incident was down the staircase of the vicinal surface along the [011] azimuth. $S_\parallel$ and $S_\perp$ are the components of the momentum transfer parallel and perpendicular to the electron beam, respectively. The specular beam was split in the $S_\parallel$ direction into two peaks around a central part, which is located within the RHEED zeroth Laue zone.

C. Terrace width growth dynamics

The use of a vicinal Si(100)-(2×1) surface as a substrate enables the study of the influence of terrace step edges on In growth by PLD. Real-time RHEED patterns were acquired in the out-of-phase diffraction condition in order to measure the average terrace width during the growth of In on Si. In the out-of-phase condition, incident electrons scattered from different surface layers destructively interfere. This results in a splitting of the specular RHEED beam for a vicinal surface when the electron beam direction has a component down the staircase. The diffracted beam profiles are sensitive to terrace periodicity and step edge disorder. Kinematical approaches were previously utilized for quantitative analysis of RHEED during thin film growth on vicinal surfaces.[39,40]

The average terrace width of the clean vicinal Si(100)-(2×1) surface is expected to be affected by chemical etching and heat cleaning. Prior to In deposition, the average terrace width of the Si(100)-(2×1) substrate was measured along the [011] azimuth. The specular beam showed split peaks at the out-of-phase condition, which is defined by $2d \sin \theta_{inc} = (n+1/2)\lambda$, where d is the monolayer step height, θ_{inc} is the incident angle corresponding to the out-of-phase condition, n is an integer, and λ is the electron wavelength. Figure 7 is a RHEED pattern of the vicinal Si(100)-(2×1) that shows splitting of the specular beam in the $S_\parallel$ direction, where $S_\parallel$ and $S_\perp$ are the components of the momentum transfer parallel and perpendicular to the electron beam, respectively. The angle of incidence θ_{inc} corresponding to the out-of-phase condition was ~65 mrad. The average terrace width was determined from the spacing of the split peaks $L = 2\pi/(d\theta)k \sin \theta_{inc}$, where $k = 47.78$ Å^{-1} is the Ewald sphere radius and $d\theta = 32.7$ mrad is the splitting angle. Taking into account the RHEED instrumental response of 0.20 ± 0.02 Å^{-1}, the average terrace width of the Si(100)-(2×1) surface was obtained to be $L = 61 \pm 10$ Å. The instrumental response was obtained from the FWHM along the specular beam in the $S_\parallel$ direction at the Bragg diffraction condition. The corresponding misorientation angle for the vicinal Si(100)-(2×1) substrate with a step height of 1.36 Å is approximately 1.3°, which is consistent with the $1.0 \pm 0.5°$ miscut angle specified by the manufacturer. The average terrace width depends on the misorientation angle from the low-index (100) plane. For a cleaned vicinal Si(100) surface tilted 4° toward [011], STM showed terraces of 40–45 Å in width.[12] No inner potential correction is needed since the interference condition in RHEED depends only on the extra external path length; a refraction correction at the top or bottom of a step would be identical and thus cancels.[39] Dynamic interaction due to surface wave resonance does not change the splitting or streak asymmetry.[41]

The temporal evolution of the terrace width during growth of In(4×3) was measured by directing the RHEED electron beam down the staircase, along the [011] azimuth of the Si surface, and line scans were taken over the splitting peaks with a frame rate of 7–8 frame/s. The split peak spacing was measured during In growth at different growth temperatures and laser energy densities. Figure 8 shows the average terrace width L during the growth of In at T_s of 358 °C. The laser was operated at a 2 Hz repetition rate with an energy density of 0.50 J/cm^2 on the In target. L decreased from 61 ± 10 to 53 ± 8 Å during the growth of the first ~11 ML of In. The width of the split peaks, which is related to defects, slightly decreased with deposition time. The inset of Fig. 8 shows RHEED intensity profiles taken across one of the split peaks, in the $S_\perp$ direction, before and during the deposition at ~1 and ~7.6 ML. The corresponding FWHMs extracted from a Lorentzian fit to the intensity profiles were 0.24, 0.21, and 0.20 Å^{-1}, respectively. The growth of In(4×3) by two different laser ablation energy densities of 0.25 and 0.50 J/cm^2 at T_s of 400 °C showed a decrease in the average terrace width to 49 ± 7 and 52 ± 8 Å, respectively, as shown in Fig. 9. The decrease in the average terrace width during growth of In indicates alternation of the terrace edge morphology.

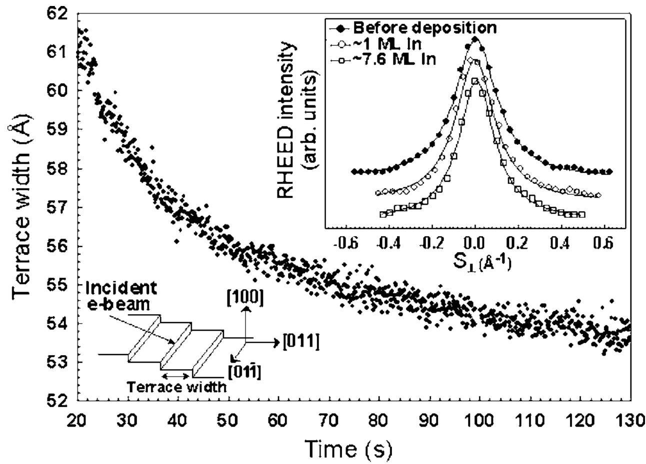

FIG. 8. The average terrace width L during growth of In at T_s of 358 °C on the vicinal Si(100)-(2×1) surface. The laser was operated at a 2 Hz repetition rate and an energy density of 0.50 J/cm^2 on the In target. The primary electron energy of 8.6 keV incident was down the staircase along the [011] azimuth of the Si surface. L was decreasing during the growth of the first ~11 ML of In. RHEED intensity profiles taken across one of the split peaks, in the $S_\perp$ direction, before and during the deposition at ~1 and ~7.6 ML are shown in the inset. The FWHM is measured from a Lorentzian fit to the intensity profiles. A schematic of a vicinal surface is shown in the inset.

The variation in the average terrace width during In growth on the vicinal Si(100)-(2×1) depends on the deposition conditions. A STM study showed step rearrangement on vicinal Si(100) induced by In adsorption and annealing.[18] At an annealing temperature of 500 °C, STM showed an increase in terrace width from 40 to ≥200 Å, which occurred by step bunching. The original step direction of [0$\bar{1}$1] changed to a preferred low-index [010] and [001] directions, and the terraces widened to ~400 Å after annealing at 510 °C.[18] By using reflection electron microcopy, step bunching on a Si(001) vicinal surface during Au deposition resulted in an increase in the terrace width with deposition time.[42] Step bunching occurs when the steps on the vicinal surface become unstable and come together to form strips of high and low step densities. This results in change in the terrace width distribution. If the RHEED electron beam is incident along the miscut direction, step bunching causes a decrease of the splitting angle $d\theta$. We observed an increase in $d\theta$ during In growth, indicating a decrease in the split peak spacing L. Previous studies showed that the average terrace width of vicinal surfaces decreased with deposition time or temperature.[43–45] Moreover, roughening or meandering at the step edges increases disorder at terrace edges, which, for a stepped surface, causes fluctuation in the terrace width.[46] If the degree of disorder were high, the electrons would effectively traverse more up and down steps along its path. This causes the diffracted beam to broaden and the staircase could be lined up in other low-index directions leading to a decrease in or a disappearance of the split peak spacing from the miscut direction of the vicinal Si surface.[46] In the present study, the split peak spacing, which is measured for the [011] azimuth, remained at its maximum with further In deposition.

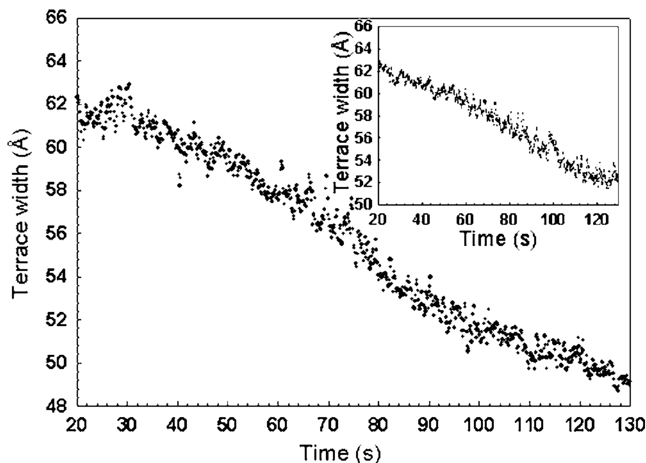

FIG. 9. The average terrace width L during femtosecond PLD of In by two different laser energy densities of 0.25 and 0.50 J/cm^2 (inset) for ablation of In target. The laser was operated at a 2 Hz repetition rate and the growth temperature T_s was 400 °C. The 8.6 keV electron beam incident was down the staircase along the [011] azimuth of the Si surface.

The change in the terrace width distribution during In growth suggests that collective surface processes occurred. The sticking probability of In on Si(100) becomes appreciably less than unity as the temperature is increased above 550 °C, at which In desorption becomes considerable.[2,47] In our study, a strong (4×3) pattern was observed at substrate temperatures of 350–420 °C. Li *et al.*[18] showed that the In(4×3) on the Si(100) terraces did not desorb at temperatures below 500 °C. This was consistent with the desorption kinetic studies of Knall *et al.*,[3] who determined that the binding energy of In on top of the (4×3) surface is lower than that of In in the (4×3) surface, 2.45 eV versus 2.85 eV, respectively, implying that it is more difficult to desorb In from a (4×3) surface than from In on top of it. The detachment of In atoms from step edges is more likely than direct desorption from the step edges because the former process generally has a smaller activation energy.[48]

In the reciprocal lattice of a vicinal surface, the split peak results from the intersection of the Ewald sphere with the lattice rods of the terrace edges. Changes in the terrace edge morphology can be qualitatively observed by the RHEED diffraction pattern. Surface atoms at step edges have lower coordination than atoms at terraces, making them less stable, particularly at high temperatures. The observed decrease in the average terrace width could be attributed to the detachment of In atoms from step edges followed by the diffusion on the terrace surface. The In atoms can then form clusters and/or desorb from the surface. A previous work by dark-field LEEM showed that rearrangement of the Si(001) surface occurred through etching of the Si surface by In at temperatures greater than 650 °C.[19] This suggests that etching by energetic In deposits preferentially occurs at terrace edges of the Si surface, which could be the cause of the observed decrease in the average terrace width at the beginning of the deposition.

Figure 10 shows the time evolution of the average terrace width L during In growth at T_s of 405 °C for a total coverage of ~38 ML. The RHEED pattern of In(4×3) taken after deposition of ~38 ML is shown in the inset of Fig. 10. The splitting of the specular beam indicates that the In film forms a staircase in the [011] azimuth of the Si surface due to

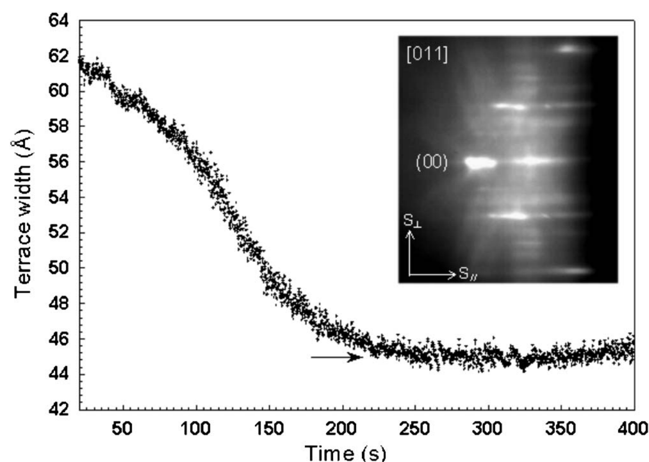

FIG. 10. The average terrace width L during growth of In by femtosecond PLD at T_s of 405 °C on the vicinal Si(100)-(2×1) surface. The laser was operated at a 2 Hz repetition rate and an energy density of 0.50 J/cm^2 on the In target. The 8.6 keV electron beam incident was down the staircase along the [011] azimuth of the Si surface. L decreased until an equilibrium reached after deposition of ~23 ML of In. The arrow indicates the equilibrium L. The In(4×3) RHEED pattern remained observable during the deposition. In the inset, RHEED pattern of In(4×3) for In coverage of ~38 ML is shown. The splitting of the specular beam was along the [011] azimuth of the vicinal Si(100) surface and parallel to the RHEED shadow edge.

the growth by step flow. The deposition was started at a time of 20 s. The laser was operated at a 2 Hz repetition rate with an energy density of 0.50 J/cm^2 on the In target. The terrace width L decreased from 61±10 Å to an equilibrium value of 45±7 Å after deposition of ~23 ML of In. From the start of the deposition until the deposition time was ~230 s, which is the range at which the terrace width was decreasing, the In(4×3) film grew by step flow. At 230 s, corresponding to a coverage of ~23 ML, the terrace width reached a steady value. Because of surface processes such as the detachment of In atoms from step edges, competition between growth by step flow and growth on surface terraces arises as the film coverage was increased. Also, with the increase in coverage, the concentration of In on surface terraces increased and the growth of the In film could be a mixture of In island formation and step flow growth over part of the surface. When the equilibrium terrace width was reached, the possibility of growth of In islands increased. At a high film coverage of more than 38 ML, the density and size of islands increased on surface terrace, which gave rise to a (1×1) RHEED pattern and disappearance of the (4×3) RHEED pattern.

IV. CONCLUSIONS

The growth of In(4×3) on the vicinal Si(100)-(2×1) surface by femtosecond PLD was studied by *in situ* RHEED within the temperature range of 350–420 °C. Unlike thermal evaporation, the energetic and pulsed nature of PLD lead to the creation of mobile In clusters, enhancing the 2D growth. The growth of the In(4×3) layers occurred by the step flow mode. The growth stages of the In(4×3) layer, which are probed by RHEED intensity relaxation, proceeds in a two-step process: formation of small In clusters and surface diffusion to the terrace step edges with a characteristic activation energy E_d and a diffusion rate constant ν_0. During growth of the In film, a reduction in the average terrace width occurred and was attributed to the detachment of In atoms from terrace edges. As the In coverage was increased, the terrace width reached an equilibrium length, where the possibility of growth of In islands increased. Observation of the RHEED pattern transition from (4×3) to (1×1) was associated with the growth of In islands on the terrace surfaces.

ACKNOWLEDGMENTS

This material is based on work supported by the U.S. Department of Energy, Division of Material Sciences, under Grant No. DE-FG02-97ER45625 and the National Science Foundation Grant No. DMR-0420304.

[1] N. Kuwata, T. Asai, K. Kimura, and M. Mannami, Surf. Sci. **143**, L393 (1984).
[2] J. Knall, J.-E. Sundgren, G. V. Hansson, and J. E. Greene, Surf. Sci. **166**, 512 (1986).
[3] J. Knall, S. A. Barnett, J.-E. Sundgren, and J. E. Greene, Surf. Sci. **209**, 314 (1989).
[4] A. A. Baski, J. Nogami, and C. F. Quate, Phys. Rev. B **43**, 9316 (1991).
[5] V. G. Kotlyar, A. V. Zotov, A. A. Saranin, T. V. Kasyanova, M. A. Cherevik, O. V. Bekhtereva, M. Katayama, K. Oura, and V. G. Lifshits, e-J. Surf. Sci. Nanotechnol. **1**, 33 (2003).
[6] V. G. Kotlyar, A. V. Zotov, A. A. Saranin, E. N. Chukurov, T. V. Kasyanova, M. A. Cherevik, I. V. Pisarenko, H. Okado, M. Katayama, K. Oura, and V. G. Lifshits, Phys. Rev. Lett. **91**, 026104 (2003).
[7] J. R. Ahn, J. H. Byun, W. H. Choi, H. W. Yeom, H. Jeong, and S. Jeong, Phys. Rev. B **70**, 113304 (2004).
[8] A. A. Saranin, A. V. Zotov, V. G. Kotlyar, H. Okado, M. Katayama, and K. Oura, Surf. Sci. **598**, 136 (2005).
[9] A. A. Saranin, A. V. Zotov, I. A. Kuyanov, M. Kishida, Y. Murata, S. Honda, M. Katayama, K. Oura, C. M. Wei, and Y. L. Wang, Phys. Rev. B **74**, 125304 (2006).
[10] A. V. Zotov, A. A. Saranin, V. G. Lifshits, J.-T. Ryu, O. Kubo, H. Tani, M. Katayama, and K. Oura, Phys. Rev. B **57**, 12492 (1998).
[11] A. A. Saranin, A. V. Zotov, V. G. Lifshits, J.-T. Ryu, O. Kubo, H. Tani, T. Harada, M. Katayama, and K. Oura, Phys. Rev. B **60**, 14372 (1999).
[12] B. E. Steele, D. M. Cornelison, L. Li, and I. S. T. Tsong, Nucl. Instrum. Methods Phys. Res. B **85**, 414 (1994).
[13] O. Bunk, G. Falkenberg, L. Seehofer, J. H. Zeysing, R. L. Johnson, M. Nielsen, R. Feidenhans'l, and E. Landemark, Appl. Surf. Sci. **123/124**, 104 (1998).
[14] O. Bunk, G. Falkenberg, J. H. Zeysing, R. L. Johnson, M. Nielsen, and R. Feidenhans'l, Phys. Rev. B **60**, 13905 (1999).
[15] N. Takeuchi, Phys. Rev. B **63**, 245325 (2001).
[16] T. M. Schmidt, J. L. P. Castineira, and R. H. Miwa, Appl. Phys. Lett. **79**, 203 (2001).
[17] P. J. E. Reese, T. Miller, and T.-C. Chiang, Phys. Rev. B **64**, 233307 (2001).
[18] L. Li, Y. Wei, and I. S. T. Tsong, Surf. Sci. **304**, 1 (1994).
[19] H. A. McKay and R. M. Feenstra, Surf. Sci. **547**, 127 (2003).
[20] A. V. Zotov, A. A. Saranin, K. V. Ignatovich, V. G. Lifshits, M. Katayama, and K. Oura, Surf. Sci. **391**, L1188 (1997).
[21] J. T. Ryu, T. Fuse, O. Kubo, T. Fujino, H. Tani, T. Harada, A. A. Saranin, A. V. Zotov, M. Katayama, and K. Oura, J. Vac. Sci. Technol. B **17**, 983 (1999).
[22] J. C. Miller and R. F. Haglund, *Laser Ablation and Desorption, Experimental Methods in the Physical Sciences* (Academic, Boston, 1998), Vol. 30.
[23] J. Shen, Z. Gai, and J. Kirschner, Surf. Sci. Rep. **52**, 163 (2004).
[24] H. Jenniches, M. Klaua, H. Hoche, and J. Kirschner, Appl. Phys. Lett. **69**, 3339 (1996).
[25] G. Koster, G. J. H. M. Rijnders, D. H. A. Blank, and H. Rogalla, Appl. Phys. Lett. **74**, 3729 (1999).
[26] H. Karl and B. Stritzker, Phys. Rev. Lett. **69**, 2939 (1992).
[27] H. T. Yang and W. S. Berry, J. Vac. Sci. Technol. B **2**, 206 (1984).
[28] M. A. Hafez and H. E. Elsayed-Ali, J. Appl. Phys. **101**, 113515 (2007).
[29] S. Martini, A. A. Quivy, T. E. Lamas, and E. C. F. da Silva, Phys. Rev. B

72, 153304 (2005).
[30]J. Choi, C. B. Eom, G. Rijnders, H. Rogalla, and D. H. A. Blank, Appl. Phys. Lett. **79**, 1447 (2001).
[31]M. Lippmaa, N. Nakagawa, M. Kawasaki, S. Ohashi, and H. Koinuma, Appl. Phys. Lett. **76**, 2439 (2000).
[32]V. S. Achutharaman, N. Chandrasekhar, O. T. Valls, and A. M. Goldman, Phys. Rev. B **50**, 8122 (1994).
[33]K. Shiramine, T. Itoh, and S. Muto, J. Vac. Sci. Technol. B **22**, 642 (2004).
[34]D. M. Zhang, L. Guan, Z. H. Li, G. J. Pan, H. Z. Sun, X. Y. Tan, and L. Li, Surf. Coat. Technol. **200**, 4027 (2006).
[35]J. Perriere, E. Millon, W. Seiler, C. Boulmer-Leborgne, V. Carciun, O. Albert, J. C. Loulergue, and J. Etchepare, J. Appl. Phys. **91**, 690 (2002).
[36]L. Bardotti, P. Jensen, A. Hoareau, M. Treilleux, and B. Cabaud, Phys. Rev. Lett. **74**, 4694 (1995).
[37]P. Deltour, J.-L. Barrat, and P. Jensen, Phys. Rev. Lett. **78**, 4597 (1997).
[38]A. Bogicevic, S. Liu, J. Jacobsen, B. Lundqvist, and H. Metiu, Phys. Rev. B **57**, R9459 (1998).
[39]C. S. Lent and P. I. Cohen, Phys. Rev. B **33**, 8329 (1986).
[40]L. Daweritz and K. Ploog, Semicond. Sci. Technol. **9**, 123 (1994).
[41]P. R. Pukite, J. M. Van Hove, and P. I. Cohen, J. Vac. Sci. Technol. B **2**, 243 (1984).
[42]H. Minoda and K. Yagi, Phys. Rev. B **60**, 2715 (1999).
[43]K. Fang, T.-M. Lu, and G.-C. Wang, Phys. Rev. B **49**, 8331 (1994).
[44]U. Hessinger, M. Leskovar, and M. A. Olmstead, Phys. Rev. Lett. **75**, 2380 (1995).
[45]M. A. Hafez and H. E. Elsayed-Ali, J. Appl. Phys. **91**, 1256 (2002).
[46]M. G. Lagally, D. E. Savage, and M. C. Tringides, in *Reflection High-Energy Electron Diffraction and Reflection Electron Imaging of Surfaces*, edited by P. K. Larson and P. J. Dobson (Plenum, New York, 1988), Vol. 188, p. 139.
[47]J. Knall, J.-E. Sundgren, J. E. Greene, A. Rockett, and S. A. Barnett, Appl. Phys. Lett. **45**, 689 (1984).
[48]K.-S. Kim, Y. Takakuwa, T. Abukawa, and S. Kono, Surf. Sci. **410**, 99 (1998).